# Numerical estimates for the bulk viscosity of ideal gases

M. S. Cramer

Citation: Physics of Fluids (1994-present) **24**, 066102 (2012); doi: 10.1063/1.4729611
View online: http://dx.doi.org/10.1063/1.4729611
View Table of Contents: http://scitation.aip.org/content/aip/journal/pof2/24/6?ver=pdfcov
Published by the AIP Publishing

PHYSICS OF FLUIDS **24**, 066102 (2012)

# Numerical estimates for the bulk viscosity of ideal gases

M. S. Cramer
*Department of Engineering Science and Mechanics, MC 0219, Virginia Polytechnic Institute and State University, Blacksburg, Virginia 24061, USA*

(Received 18 January 2012; accepted 9 April 2012; published online 28 June 2012)

We estimate the bulk viscosity of a selection of well known ideal gases. A relatively simple formula is combined with published values of rotational and vibrational relaxation times. It is shown that the bulk viscosity can take on a wide variety of numerical values and variations with temperature. Several fluids, including common diatomic gases, are seen to have bulk viscosities which are hundreds or thousands of times larger than their shear viscosities. We have also provided new estimates for the bulk viscosity of water vapor in the range 380–1000 K. We conjecture that the variation of bulk viscosity with temperature will have a local maximum for most fluids. The Lambert-Salter correlation is used to argue that the vibrational contribution to the bulk viscosities of a sequence of fluids having a similar number of hydrogen atoms at a fixed temperature will increase with the characteristic temperature of the lowest vibrational mode. © *2012 American Institute of Physics*. [http://dx.doi.org/10.1063/1.4729611]

## I. INTRODUCTION

Shear viscosity plays a central role in the study of fluid dynamics. Ultimately, it is the source of all forms of loss and drag and gives rise to the instabilities which lead to flow turbulence. As a result, its molecular interpretation, variation with temperature and pressure, and numerical values can be found in nearly every reference on fluid mechanics. In contrast, the general understanding of the second or bulk viscosity

$$\mu_b \equiv \lambda + \frac{2}{3}\mu \tag{1}$$

is considerably less developed. Here $\mu_b = \mu_b(p, T), \lambda = \lambda(p, T)$, and $\mu = \mu(p, T)$ are the bulk, second, and shear viscosities, respectively. The quantities $T$ and $p$ are the absolute temperature and pressure. The theoretical foundation of an equilibrium, i.e., zero-frequency, bulk viscosity has been known for over half a century. One of the first detailed studies is due to Tisza[1] who related the bulk viscosity to molecular energy storage and showed how the second and bulk viscosities found in the Navier-Stokes equations are obtained in the equilibrium limit. Further discussions of the relation of the bulk viscosity to classical fluid dynamics are found in Graves and Argrow[2] and Herzfeld and Litovitz.[3] However, experimental data for $\mu_b$ are restricted to only a few fluids for a limited temperature range; see, e.g., the compilations by Karim and Rosenhead,[4] Thompson,[5] and Graves and Argrow.[2] The main goal of the present study is to extend the current data set as well as to illuminate the different temperature variations possible for $\mu_b$.

Because the second and bulk viscosities are fundamental transport properties necessary for the full specification of the Navier-Stokes stress tensor, their values and variations with the thermodynamic variables are of obvious scientific interest. In addition, many technological applications involve complex, fully viscous and compressible flows which can only be described numerically. Accurate descriptions of such flows therefore require reasonably accurate estimates for the bulk viscosity. Examples include the flows in Rankine cycle power systems using steam as a working fluid as well as systems which employ non-aqueous working fluids. The latter working fluids tend to be advantageous when non-fossil fuel heat sources are used; see, for example, the studies of organic Rankine cycles by Curran,[6] Devotta and Holland,[7] Yan,[8] Hung, Shai, and Wang,[9] Liu, Chien, and

 

Wang,[10] Wei *et al.*,[11] Saleh *et al.*,[12] and Shuster, Karellas, and Aumann[13] or the studies of Dostal *et al.*,[14,15] Dostal,[16] Moisseytsev,[17] Moisseytsev and Sienicki,[18] and Sarkar[19,20] on the use of $CO_2$ and $N_2O$ for nuclear power systems. Even if the working fluid is steam, our examination of the literature indicates that no estimates of the bulk viscosity are currently available for water vapor. We believe that the present study provides the first explicit estimate of the bulk viscosity of water vapor. Other applications involving complex molecules and configurations include wind tunnel similarity studies and nanoparticle generation in the pharmaceutical industry. Examples of the former are the studies of $SF_6$ as a wind tunnel fluid by Anderson[21,22] and Anders[23] to obtain a better match of Mach and Reynolds numbers between test and flight conditions. In the pharmaceutical industry, the rapid expansion of supercritical solution (RESS) process expands a dilute supersaturated mixture of a desired precipitate in a pressurized solvent, typically $CO_2$, through a capillary nozzle resulting in a precipitate of relatively uniform diameter; see, e.g., Tom and Debenedetti,[24] Eckert *et al.*,[25] and Turk *et al.*[26]

The present study will focus on the estimation of the bulk viscosity for low pressure or dilute gases. Thus, the equation of state is the well known ideal gas law

$$p = \rho RT, \tag{2}$$

where $R$ is the gas constant and $\rho$ is the fluid density. As a result of the simplicity of (2), the energy per unit mass is a function of temperature only and can be written as the sum

$$e = e(T) = e_{tr} + \sum_{i=1}^{N} e_i,$$

where $e_{tr}$ is the molecular translational energy and the $e_i$ are the contributions due to the $N$ internal energy modes, i.e., the energies associated with molecular rotation and vibration.

If the gas is monatomic, e.g., He, Ar, or Ne, the rotational and vibrational energies are regarded as negligible and changes to the gas are rapidly communicated by way of molecular collisions. Because a new equilibrium state is established within a few collisions, the time scale for the establishment of translational equilibrium is taken to be $\tau_c \equiv$ the average time between collisions. If the gas is polyatomic, changes in the internal energy modes are also driven by collisions. However, the probability that any particular collision results in a change in the rotational or vibrational state of either molecule depends on the details of the collision and the translational energy of collision relative to the lowest energy state of each internal mode. Thus, the number of collisions required to bring the internal energy modes into equilibrium with each other and with the translational modes may be more, sometimes many more, than the number required to establish translational equilibrium. The time scale associated with this process will be denoted as $\tau_i$ and will be referred to as the relaxation time for the $i$th internal mode. The relation of the bulk viscosity to these relaxation times was first established by Tisza.[1] In the notation used here, Tisza's near-equilibrium, i.e., zero-frequency, result can be written

$$\mu_b = (\gamma - 1)^2 \sum_{i=1}^{N} \frac{c_{vi}}{R} p\tau_i, \tag{3}$$

where

$$c_{vi} = c_{vi}(T) \equiv \frac{de_i}{dT} \tag{4}$$

is the isochoric specific heat associated with each internal mode and $\gamma = \gamma(T)$ is the ratio of specific heats. In the ideal gas limit considered here

$$\mu_b(p, T) \to \mu_b(T)$$

and each $p\tau_i = f(T)$ only. Tisza's result (3) is completely consistent with the idea that $\mu_b \equiv 0$ for monatomic gases for which all $c_{vi}$ are taken to be zero. Furthermore, when the temperature is so low that the energy of collision is considerably lower than the energy associated with the $i$th energy mode, $c_{vi} \approx 0$ and the $i$th mode makes no significant contribution to the bulk viscosity. Since Tisza's paper

appeared, more sophisticated derivations of (3) have been carried out. A comprehensive discussion and review may be found in the text by Chapman and Cowling.[27]

Previous estimates of the bulk viscosity of dilute gases have either used direct methods such as acoustic absorption measurements or have measured the relaxation time $\tau_i$ and then used (3) to deduce $\mu_b$. One of the earliest studies to estimate $\mu_b$ directly from acoustic absorption data is that of Karim and Rosenhead,[4] albeit for liquid, rather than gaseous, water. More recent estimates based on absorption are due to Prangsma, Alberga, and Beenakker[28] for low pressure $N_2$, CO, $CH_4$, and $CD_4$ who found values of $\mu_b = 0.73\ \mu$, $0.55\ \mu$, $1.33\ \mu$, and $1.17\ \mu$ at 293 K, respectively. A second direct method is to infer the bulk viscosity from measurements of shock thickness. The latter method was used by Sherman[29] to deduce that $\mu_b \approx 0.67\ \mu$ for low pressure $N_2$. In both direct methods, the dilation rates must be low enough to ensure that the fluid is in local thermodynamic equilibrium (LTE) which, in turn, ensures the validity of the Navier-Stokes-Fourier equations. In the case of shock thickness measurements, it can be argued that LTE is guaranteed if the shock is weak. In the case of acoustic absorption the condition $\omega\tau_i|_{\max} \ll 1$, where $\omega$ is the acoustic frequency, is required. A significant advantage of the indirect method used here is that we only need accurate estimates of $\tau_i$ regardless of the frequency employed in its experimental determination. Substitution of the estimate for $\tau_i$ in (3) guarantees that the resultant estimate for $\mu_b$ is the desired zero-frequency transport property.

The first to apply (3) to estimate the low frequency bulk viscosity was Tisza[1] who estimated that $\mu_b$ is roughly 2000 times $\mu$ for both $CO_2$ and $N_2O$. Tisza also estimated that $\mu_b = 0(\mu)$ for air. More recent computations based on (3) were given by Emanuel[30] who gave $\mu_b \approx 3000\ \mu$ for $CO_2$ at 303 K.

Efforts to estimate $\tau_i$ have also included theoretical studies. For example, Parker[31] carried out a classical analysis to derive the following expression for the rotational relaxation times of diatomic gases:

$$Z_r \equiv \frac{\tau_r}{\tau_c} = Z_r^{\infty} \frac{4T'}{\pi(4+\pi) + 2\pi^{\frac{3}{2}}(T')^{\frac{1}{2}} + 4T'}, \tag{5}$$

where $Z_r^{\infty}$ is a nondimensional constant dependent on parameters characterizing the molecular interaction potential, $T' \equiv Tk/\epsilon'$, $k$ is Boltzmann's constant, $\tau_r$ is the rotational relaxation time, and $\epsilon'$ is an energy characterizing the intermolecular potential used by Parker. The quantity $Z_r$ is the collision number representing the number of collisions required to obtain rotational equilibrium. Parker's result corresponds to a gradual increase of $Z_r$ with increasing temperature. If we assume the rotational mode is fully activated and that the vibrational portion of the specific heat is negligible so that $\gamma - 1 = R/c_v = 2/(f_r + 3)$ and if we estimate the viscosity by the exact hard-sphere model, i.e.,

$$\mu = \mu_{HS} = \frac{5}{4} p\tau_c, \tag{6}$$

we find that the rotational part of $\mu_b$ can be written

$$\frac{\mu_b}{\mu_{HS}} = \frac{8 f_r}{5(f_r+3)^2} Z_r, \tag{7}$$

where $f_r$ denotes the number of relevant rotational modes. Because $f_r =$ constant, the temperature variation of $\mu_b/\mu$ is therefore expected to be the same as $Z_r$. If we employ the more accurate estimate for shear viscosity described in Sec. II, the increase in $\mu_b/\mu$ with $T$ suggested by (7) will be somewhat weakened.

One of the best known classical theories for vibrational relaxation is the Landau-Teller theory. An easily accessible description of the Landau-Teller theory can be found in Herzfeld and Litovitz.[3] Landau-Teller theory is expected to be valid at temperatures which are so large that the long range attractive intermolecular forces are negligible during collisions. The repulsive part of the intermolecular potential was taken to be of the form $V_o \exp(\alpha r)$, where the constants $V_o$ and $\alpha$ give a measure of the magnitude and steepness of the potential. The result of Landau and Teller's analysis

is that

$$Z_{10} \approx \text{constant}\, e^{\eta^{\frac{1}{3}}}, \tag{8}$$

where

$$\eta = \text{constant} \cdot \frac{m_e v^2}{\alpha^2 kT}. \tag{9}$$

In (9) the constant is a pure number, $\nu$ is the lowest vibration frequency, and $m_e$ is the effective molecular mass. The quantity $Z_{10}$ represents the number of collisions required for a transfer of translational energy to the lowest vibrational mode. The relation of $Z_{10}$ to the vibrational relaxation time $\tau_v$ is

$$Z_v \equiv \frac{\tau_v}{\tau_c} = \frac{Z_{10}}{1 - e^{-\frac{\theta_v}{T}}}. \tag{10}$$

The factor in the denominator of (10) accounts for the fact that collisions with molecules in the same vibrational state will result in no energy transfer. The constant $\theta_v$ is the characteristic temperature associated with the lowest vibrational energy level. It can be shown that $\eta$ is proportional to the square of the ratio of the duration of collision ($t_d$) to the period of vibration of the lowest mode ($t_v \equiv \nu^{-1}$). Thus, at these temperatures, $Z_{10}$ will decrease monotonically with increasing temperature.

Although (8)–(9) formally holds for only sufficiently large temperatures, experimental data for $Z_v$ and $p\tau_v$ frequently fit straight line relations

$$\log_{10} Z_v \text{ or } \log_{10} p\tau_v = \text{constant} + \text{constant} \cdot T^{-\frac{1}{3}} \tag{11}$$

over a wide range of temperatures. Such a relation is used in many published curve-fits and will be employed for some of the fits presented here.

We note that the rapid decrease of $Z_v$ with $T$ suggested by (8)–(10) is likely to be stronger than any increase in the coefficient of $p\tau_i$ with temperature; see, e.g., the discussion of Sec. II. Because the shear viscosity of dilute gases increases with temperature, we should therefore expect both $\mu_b$ and the ratio $\mu_b/\mu$ to ultimately decrease as the temperature increases when the Landau-Teller law holds.

At lower temperatures, forces neglected in the Landau-Teller theory become important. Models which include attractive forces were first described by Schwartz, Slawsky, and Herzfeld,[32] Schwartz and Herzfeld,[33] and Tanczos;[34] see, also, Herzfeld and Litovitz[3] for a comprehensive summary. The role of the long range attractive force is to increase the relative speed of the colliding particles, therefore decreasing $t_d$ resulting in a more efficient transfer of energy from translation to vibration. Under these conditions, the Landau-Teller asymptote overpredicts the value of $Z_v$ and the vibrational relaxation time. When the temperature is so low that the molecular kinetic energy is on the order of or much less than the minimum in the intermolecular potential, molecules can pair to form dimers which further increases the efficiency of the energy exchange and decreases the vibrational relaxation time; see, e.g., the discussion by Lambert.[35] As the temperature increases, the relative velocity of collision increases and dimers are less likely to form. Thus, at sufficiently low temperatures, the values of $Z_v$ and vibrational relaxation times are expected to increase with increasing temperature. We would therefore expect the values of $Z_v$, $p\tau_v$, and the bulk viscosity to have a local maximum as the energy exchange process shifts from the low temperature increase with temperature to the strong decrease with temperature associated with the high temperature Landau-Teller regime.

When we consider polar fluids the additional effect of the dipole forces must be considered, particularly when the kinetic energy is on the order of or smaller than the energy associated with the dipole. At such temperatures, the dipoles tend to re-orient the molecules during the collision. The additional forces and the alignment of the dipoles yield a very efficient translational-vibrational energy transfer and the resultant vibrational relaxation times tend to be smaller than those of non-polar fluids. Thus, the bulk viscosities of polar fluids are also expected to be smaller than those of non-polar fluids. Furthermore, full re-alignment is less likely to occur as the molecular speeds increase. As a result, the values of $Z_v$ and $\tau_v$ will increase with temperature. At higher temperatures, re-orientation does not have time to occur, the repulsive force dominates, and the Landau-Teller

theory will ultimately hold. Again, the variation of $Z_v$, $\tau_v$, and $\mu_b$ with temperature is expected to exhibit a local maximum.

The aforementioned theories, and even their extensions, cannot yet provide accurate and comprehensive predictions of the relaxation times. Here our primary goal is to provide numerical estimates of the bulk viscosity for a variety of common fluids. We will also give simple formulas for the temperature variation of $\mu_b$ which can provide future researchers with formulas for use in design and computational studies. Hence, we will simply use the physics described above to interpret our results for the bulk viscosity and, in some cases, to guide our choices for curve-fits.

## II. ASSUMPTIONS AND MODELS

In all that follows, we will assume that the rotational and vibrational modes relax independently, that all the rotational modes relax with a single relaxation time and all the vibrational modes also relax with a single time. Equation (3) can therefore be written as

$$\mu_b = \mu_b\big|_r + \mu_b\big|_v \tag{12}$$

with

$$\mu_b\big|_r \equiv (\gamma - 1)^2 \frac{f_r}{2} p\tau_r, \tag{13}$$

$$\mu_b\big|_v \equiv (\gamma - 1)^2 \frac{c_v\big|_v}{R} p\tau_v, \tag{14}$$

where $(\,)|_r$ and $(\,)|_v$ will denote rotational and vibrational contributions to the indicated quantity. Here $f_r$ = the number of rotational degrees of freedom with

$$f_r = \begin{cases} 2 \text{ for linear molecules} \\ 3 \text{ otherwise,} \end{cases}$$

and $\tau_r$ = rotational relaxation time. The quantity

$$\frac{c_v\big|_v}{R} = \frac{c_v}{R} - \frac{f_r + 3}{2} \tag{15}$$

is the vibrational part of the scaled specific heat at constant volume. The quantity $\tau_v$ is the vibrational relaxation time. Within the experimental resolution currently available, many molecules satisfy the condition of a single relaxation time. However, the vibrational modes of some molecules, e.g., $SO_2$, are known to possess distinct relaxation times.

Implicit in Eq. (13) is the assumption that the rotational modes are fully activated at the temperatures under consideration. This assumption is reasonable because most characteristic temperatures for rotation (denoted by $\theta_r$) are only a few degrees Kelvin. The primary exception is $n - H_2$ for which $\theta_r \approx 88$ K. Although one should include the rotational contribution to $\mu_b$ at most temperatures, $\tau_r$ is typically only a few collision times and is normally much smaller than $\tau_v$. Hence, if the vibrational modes are active, i.e.,

$$\frac{c_v\big|_v}{R} = O(1),$$

we will estimate the bulk viscosity using only the vibrational mode, i.e., $\mu_b \approx \mu_b\big|_v$. On the other hand, when the temperature is much less than the characteristic temperature for the lowest vibrational mode (denoted by $\theta_v$), no significant translational-vibrational energy can be exchanged and we will estimate $\mu_b$ based on the rotational contribution (13) only. An important exception here is our estimate for the bulk viscosity of water vapor where both rotational and vibrational contributions will be included. The use of only one term or the other in (12) will clearly yield a lower bound for the true value of $\mu_b$ for the substance under consideration.

Data for the specific heats are readily available for the substances of interest here. In all that follows we will compute these from the polynomial curve-fit provided by Reid, Prausnitz, and

Poling.[36] In particular, the coefficients for their curve-fit for each fluid are those given in Appendix A of their book.

In this study, the estimates for $\mu_b$ will be presented as the ratio $\mu_b/\mu$, where $\mu$ is the shear viscosity. To calculate $\mu = \mu(T)$ we use the well known Chapman-Cowling result:

$$\mu = \frac{5}{16}\left(\frac{k}{\pi \tilde{N}}\right)^{\frac{1}{2}} \frac{(WT)^{\frac{1}{2}}}{\sigma^2 \Omega}, \tag{16}$$

where $W$ is the molecular weight, $\sigma$ is the molecular diameter, $k$ is Boltzmann's constant, and $\tilde{N}$ is Loschmidt's number $= 6.0225 \times 10^{26} (\mathrm{kg\,mol})^{-1}$. The quantity $\Omega = \Omega(T)$ is the collision integral based on the 12-6 Lennard-Jones potential and is computed from

$$\Omega_{LJ} = A_1 T_*^{-A_2} + A_3 e^{-A_4 T_*} + A_5 e^{-A_6 T_*}, \tag{17}$$

$$\Omega = \Omega_{LJ} + \frac{0.2\delta^2}{T_*}, \tag{18}$$

where

$$T_* \equiv T/T_\epsilon,$$
$$T_\epsilon \equiv \frac{\epsilon}{k},$$
$$\delta \equiv \frac{\mu_p^2}{2\epsilon\sigma^3},$$

$\epsilon$ is the characteristic energy of the Lennard-Jones potential and $\mu_p$ is the molecular dipole moment. The second term in (18) represents the Stockmayer correction for polar fluids; details of the latter can be found in Reid, Prausnitz, and Sherwood.[37] A further discussion of (16)–(18) and the numerical values of $A_i, i = 1 \to 6$, are found in Reid, Prausnitz, and Poling.[36] The numerical values of $T_\epsilon$ and $\sigma$ were taken from Appendix B of Reid, Prausnitz, and Poling[36] or Svehla's original report.[38] The values of $W$ and $\mu_p$ were also obtained from Reid, Prausnitz, and Poling's[36] Appendix A.

Because $\gamma - 1 = R/c_v$ in the dilute gas limit employed here, we can use (15) to show that the coefficient of $p\tau_v$ in (14) is

$$\Delta \equiv (\gamma - 1)^2 \frac{c_v\big|_v}{R} = \frac{\frac{c_v\big|_v}{R}}{\left(\frac{f_r + 3}{2} + \frac{c_v\big|_v}{R}\right)^2}, \tag{19}$$

from which it is clear that $\Delta$ is proportional to $c_v\big|_v$ as $c_v\big|_v/R \to 0$ and that $\Delta \to 0$ as $c_v\big|_v/R \to \infty$. It is also easily verified that $\Delta$ vs $(c_v/R)\big|_v$ curves have a local maximum at

$$\frac{c_v\big|_v}{R} = \frac{f_r + 3}{2}, \quad \frac{c_v}{R} = f_r + 3$$

and the corresponding maximum value of $\Delta$ is

$$\Delta_{\max} = \frac{1}{2(f_r + 3)} = \begin{cases} \frac{1}{10} \text{ for } f_r = 2 \\ \frac{1}{12} \text{ for } f_r = 3. \end{cases}$$

Thus, any fluid for which

$$c_v > (f_r + 3)R$$

will also have a local maximum in the coefficient $\Delta$ at the temperature for which $c_v = (f_r + 3)R$. We note that the value of $c_v$ for diatomic molecules varies monotonically from $5R/2$ to $7R/2 < 5R$ and

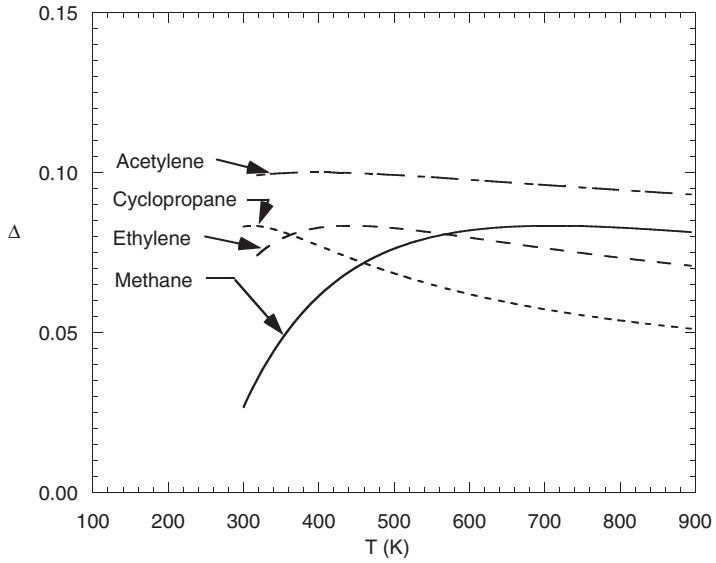


FIG. 1. Temperature variation of Δ for selected fluids.

no local maximum will be observed. For diatomic molecules, Δ will simply approach the limiting value of 4/49 < 1/12 as $T \to \infty$. Thus, $\Delta \leq 1/10$ and the vibrational contribution to $\mu_b\big|_v$ will always be less than one-tenth of the value of $p\tau_v$. To illustrate the resultant temperature variation, we have plotted Δ vs $T$ for acetylene ($f_r = 2$), cyclopropane ($f_r = 3$), ethylene ($f_r = 3$), and methane ($f_r = 3$) in Figure 1. Inspection of Figure 1 reveals relatively small values of Δ for methane for $T \approx 300$ K. The small values of Δ are due to the relatively low characteristic temperature for vibration ($\theta_v \approx 1880$ K); in fact, $c_v\big|_v \approx 0$ by $T = 257$ K. The significance of this decrease on the vibrational portion of the bulk viscosity of $CH_4$ will be discussed in Secs. IV and V.

In Secs. III and IV, the sources of data for the relaxation times are described. Many of these sources present their data graphically rather than in tabular form. Because the original numerical values are frequently unavailable, we have extracted the data from many sources using a commercial graph digitizer. For plotting purposes and the convenience of future researchers, we then fit the extracted discrete data to various analytical formulas. These fits were always based on a conventional least-squares algorithm.

## III. FLUIDS HAVING MODERATE BULK VISCOSITY

The temperature variation of $\mu_b/\mu$ for a selection of fluids having $\mu_b = O(\mu)$ is depicted in Figure 2. The characteristic temperatures for the lowest vibrational modes of nitrogen ($N_2$), carbon monoxide (CO), and methane ($CH_4$) are approximately 3360 K, 3090 K, and 1880 K, respectively. We will therefore assume that the primary contribution to $\mu_b$ is that due to rotation, at least over the temperature range of the plot. This assumption would seem reasonable for $N_2$ and CO. However, an inspection of Figure 1 and the calculations of Sec. IV lead us to conclude that there will be some non-zero contribution of the vibrational mode to the total bulk viscosity of $CH_4$ at 300 K. Nevertheless, in this section we will present our results for the rotational contribution to the bulk viscosity of $CH_4$ without a detailed consideration of $\mu_b\big|_v$. The data for the bulk viscosities of CO and $CH_4$ were taken directly from the results reported by Prangsma, Alberga, and Beenakker[28] and, following Emanuel,[39] fit to the following power-law representation:

$$\mu_b = \mu_{br}\left(\frac{T}{T_r}\right)^n, \tag{20}$$

where $\mu_{br}$, $T_r$, $n$ are constants. For $N_2$ the data of Prangsma, Alberga, and Beenakker[28] were also employed, but were supplemented by the data for $p\tau_r$ of Winter and Hill[40] at 773 K and 1073 K;

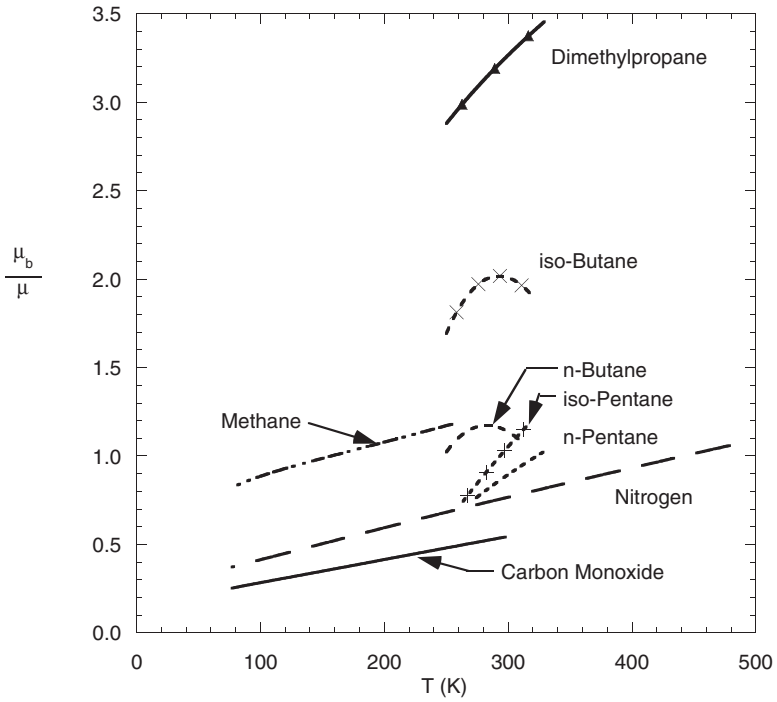


FIG. 2. Temperature variation of $\mu_b/\mu$ for fluids having moderate bulk viscosity.

these latter data were substituted into (13) to compute $\mu_b$ and the complete data set was fit to a power-law of the form (20). The values of $\mu_{br}$, $T_r$, and $n$ used for the plots of Figure 2 are

$$\mu_{br} = 0.778 \times 10^{-5}\,\text{kg/(m s)},\ T_r = 200\,\text{K},\ n = 1.376 \text{ for } N_2,$$
$$\mu_{br} = 0.533 \times 10^{-5}\,\text{kg/(m s)},\ T_r = 200\,\text{K},\ n = 1.461 \text{ for CO},$$
$$\mu_{br} = 0.836 \times 10^{-5}\,\text{kg/(m s)},\ T_r = 200\,\text{K},\ n = 1.295 \text{ for } CH_4.$$

The formal range of validity for the curve-fits for CO and $CH_4$ is 77–293 K and the formal range of validity for the $N_2$ curve-fit is expected to be 77–1073 K. In spite of the fact that the formal upper bound on the range of validity of the $CH_4$ fit is 293 K, we have truncated the curve plotted in Figure 2 at $T = 257$ K which is the temperature at which we found $\Delta \to 0$.

The bulk viscosities and $\mu_b/\mu$ for CO, $CH_4$, and $N_2$ are seen to increase gradually with temperature and the results for $N_2$ and CO are in agreement with values commonly quoted, e.g., $\mu_b \approx 0.73\ \mu$ for $N_2$ at 293 K. The gradual increase of $\mu_b/\mu$ is seen to be in qualitative agreement with the increase inherent in (5) and (7).

The remainder of the bulk viscosities plotted in Figure 2 are due to the vibrational modes only. For dimethylpropane we simply used the curve-fit provided by Ewing *et al.*[41]

$$\mu_b = A + BT, \tag{21}$$

who suggested $A = -12.9 \times 10^{-6}\,\text{kg/(m s)}$ and $B = 0.122 \times 10^{-6}\,\text{kg/(m s K)}$ and is expected to be valid for $250\,\text{K} \le T \le 325\,\text{K}$. The plots for *n*-pentane, and iso-pentane were generated by fitting a straight line to the $\rho\tau_v$ vs $T$ data of Ewing, Goodwin, and Trusler,[42] and Ewing and Goodwin,[43] respectively. The straight line fits for $\rho\tau_v$ were then converted to equations for $p\tau_v$ as follows:

$$p\tau_v = RT(\rho\tau_v) = AT + BT^2. \tag{22}$$

The values of $p\tau_v$ were then combined with (12), neglecting $\mu_b|_r$, to determine the variation of $\mu_b$ with $T$. The values of $A$ and $B$ in (22) were found to be

$$A = -4.594 \times 10^{-7}\,\text{kg/(m s K)},\ \ B = 2.671 \times 10^{-9}\,\text{kg/(m s K}^2\text{)}\ \text{for } n\text{-pentane},$$

$$A = -8.177 \times 10^{-7}\,\text{kg/(m s K)},\ \ B = 4.190 \times 10^{-9}\,\text{kg/(m s K}^2\text{)}\ \text{for iso-pentane},$$

which correspond to the authors' data in the ranges $270\,\text{K} \le T \le 330\,\text{K}$, and $260\,\text{K} \le T \le 320\text{K}$, respectively.

Data for $n$-butane and iso-butane were taken from Ewing *et al.*[44] and Ewing and Goodwin.[45] The data for $n$-butane showed evidence of a local maximum in $\mu_b$ and the data for iso-butane showed evidence of a local maximum in $\rho\tau_v$. Hence, these quantities were fit with second-order polynomials of the form

$$\mu_b = A_n + B_n T + C_n T^2 \ \text{for } n\text{-butane}, \tag{23}$$

$$\rho\tau_v = A_{\text{iso}} + B_{\text{iso}} T + C_{\text{iso}} T^2 \ \text{for iso-butane}, \tag{24}$$

where

$$A_n = -7.05 \times 10^{-5}\,\text{kg/(m s)},\ \ B_n = 5.28 \times 10^{-7}\,\text{kg/(m s K)},\ \ C_n = -8.85 \times 10^{-10}\,\text{kg/(m s K}^2\text{)},$$

$$A_{\text{iso}} = -3.412 \times 10^{-4}\,\text{(kg s)/m}^3,\ \ B_{\text{iso}} = 2.584 \times 10^{-6}\,\text{(kg s)/(m}^3\,\text{K)},$$

$$C_{\text{iso}} = -4.234 \times 10^{-9}\,\text{(kg s)/(m}^3\,\text{K}^2\text{)}.$$

The fits (23) and (24) are expected to be valid for 250 K to 310 K and 250 K to 320 K, respectively. The computed values of $\mu_b$, based on (23)–(24), for $n$-butane and iso-butane are plotted in Figure 3 along with the values of $\mu_b$ based on the authors' discrete experimental data for $\mu_b$ and $\rho\tau_v$. The scatter seen in Figure 3 is also typical of that for $n$-pentane, iso-pentane, and dimethylpropane.

The computed values of $\mu_b/\mu$ for $n$-butane, iso-butane, $n$-pentane, iso-pentane, and dimethylpropane appear to correspond to the low temperature behavior described in Sec. I. That is, the vibrational relaxation times are relatively small and increase with increasing temperature.

Because the vibrational contribution to $\mu_b/\mu$ is of order one for the fluids shown in Figure 2, it is natural to ask whether the rotational contribution to $\mu_b$ will have a significant impact on the total

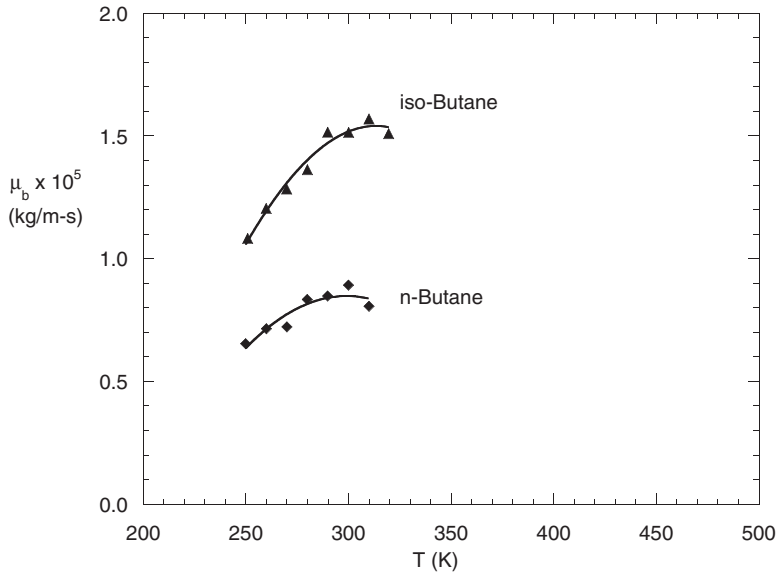


FIG. 3. Temperature variation of $\mu_b$ for iso-butane and n-butane. Solid lines denote our quadratic curve-fit and symbols denote values based on the experimental data of Ewing *et al.*[44] and Ewing and Goodwin.[45]

$\mu_b$. The relative size of these contributions is given by

$$\frac{\mu_b\big|_r}{\mu_b\big|_v} = \frac{f_r}{2}\frac{1}{\frac{c_v}{R} - \frac{f_r+3}{2}}\frac{Z_r}{Z_v}. \tag{25}$$

As an example, we consider $n$-pentane ($f_r = 2$) at 300 K. We find that $c_v = 13.53R$, $\gamma - 1 = R/c_v \approx 0.074$, $\Omega \approx 1.7$, $\mu_b\big|_v \approx 0.8953\,\mu$. Thus, at 300 K, we have

$$Z_v \approx \frac{5}{4(\gamma-1)^2\Omega\dfrac{c_v\big|_v}{R}}\frac{\mu_b\big|_v}{\mu} \approx 10.9$$

and, from (25), we have

$$\frac{\mu_b\big|_r}{\mu_b\big|_v} \approx \frac{1}{120}Z_r.$$

Thus, if $Z_r \leq 5$, $\mu_b|_r$ will be less than 4% of $\mu_b\big|_v$. As a second example, we consider dimethylpropane at 300 K. By the same analysis as for $n$-pentane, we find that $Z_v \approx 55.3$ and

$$\frac{\mu_b\big|_r}{\mu_b\big|_v} \approx \frac{Z_r}{395}.$$

Holmes, Jones, and Lawrence[46] report a value of $Z_r \approx 3.7$ which suggests that the $\mu_b|_r$ is only 0.1% of $\mu_b\big|_v$ for dimethylpropane at 300 K. When we carry out the same calculations for $n$-butane, iso-pentane, and iso-butane we find that these yield similar estimates for $\mu_b|_r/\mu_b|_v$. We would therefore expect that the results plotted in Figure 2 will change very little if the rotational contribution to $\mu_b$ is included.

Data for the relaxation times of water vapor are surprisingly scant, are frequently scattered, and are sensitive to the effects of impurities. A discussion of many of the best known studies of sound absorption and relaxation times in water vapor has been provided by Bass, Olsen, and Amme[47] and Keeton and Bass.[48] The estimates for $\mu_b/\mu$ presented here were computed using the data for $Z_v \equiv \tau_v/\tau_c$ and $Z_r \equiv \tau_r/\tau_c$ provided by Bass, Olsen, and Amme.[47] We assumed that Bass, Olsen, and Amme computed their $Z_r$ and $Z_v$ using the hard sphere collision time given by

$$\tau_c^{-1} = 4n\sigma_*^2\sqrt{\pi RT}, \tag{26}$$

where $n$ = number density and $\sigma_*$ is their value of the molecular diameter of $H_2O$. By combining (12)–(14), (16), and (26) we obtain

$$\frac{\mu_b}{\mu} = \frac{4}{5}\Omega(\gamma-1)^2\left[\frac{f_r}{2}Z_r + \frac{c_v\big|_v}{R}Z_v\right], \tag{27}$$

where we have assumed that Bass, Olsen, and Amme took the hard sphere molecular diameter $\sigma_*$ to be the same as that reported by Svehla,[38] i.e., $\sigma_* = \sigma = 2.641$ Å. The values of $Z_v$ were fit to the data presented in Figure 10 of Bass, Olsen, and Amme[47] yielding

$$Z_v = 0.003186\exp\left(\frac{76.4}{T^{\frac{1}{3}}}\right), \tag{28}$$

where $T$ is in degrees Kelvin. In this fit only the authors' six measured points between 380 K and 1000 K were used. The rotational collision number was obtained by fitting the data in the authors' Figure 11 to

$$Z_r = 29.31 - \frac{133.1}{T^{\frac{1}{3}}} \tag{29}$$

using the seven points between 380 K and 1000 K. The fit (28) is seen to be consistent with the Landau-Teller law (11) but, due to the degree of scatter, we regard (28) only as a convenient fit. Bass, Olsen, and Amme[47] and Lambert[35] suggest that there may be a local maximum in $Z_v$ at lower temperatures. Thus, (28) should be used with caution as $T \to 300$ K.

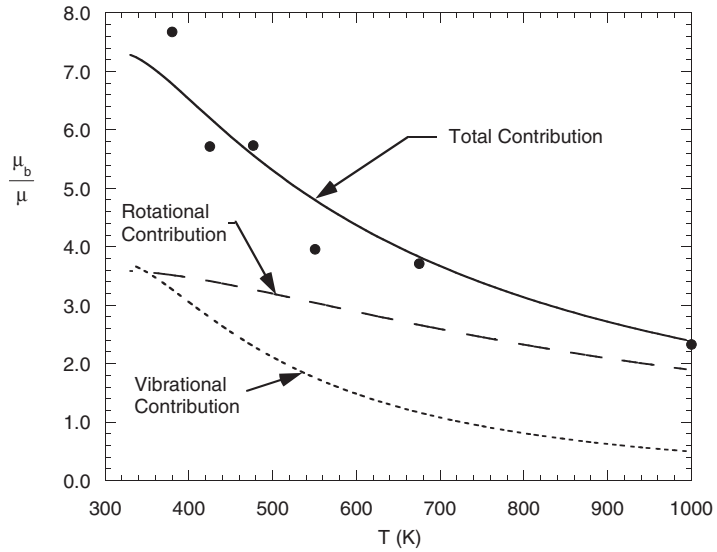


FIG. 4. Temperature variation of $\mu_b/\mu$ for water vapor. The solid line represents our curve-fit for $\mu_b/\mu$, the long dashed line represents the rotational contribution to $\mu_b/\mu$, and the short dashed line represents the vibrational contribution to $\mu_b/\mu$. Symbols denote the values of the total $\mu_b/\mu$ based on the experimentally determined values of $Z_r$ and $Z_v$ of Bass, Olsen, and Amme.[47]

The resultant variation of $\mu_b/\mu$ is plotted in Figure 4 along with the rotational and vibrational contributions to $\mu_b/\mu$, i.e.,

$$\frac{\mu_b|_r}{\mu} \equiv \frac{2}{5}\Omega(\gamma-1)^2 f_r Z_r,$$

$$\frac{\mu_b|_v}{\mu} \equiv \frac{4}{5}\Omega(\gamma-1)^2 \frac{c_v|_v}{R} Z_v.$$

In order to illustrate the scatter in the data we have also included the estimates for $\mu_b/\mu$ based on Bass, Olsen, and Amme's reported $Z_r$ and $Z_v$ at their common temperature set. In order to identify the approximate temperature at which contributions of the rotational and vibrational modes are equal we have extended our curve-fits to 330 K in Figure 4. Inspection of Figure 4 reveals that $\mu_b/\mu$ for $H_2O$ decreases with increasing temperature. The rotational contribution to $\mu_b/\mu$ is also seen to decrease with increasing temperature in spite of the fact that $Z_r$ increases with temperature. The increase of $Z_r$ is rather weak and the increase in $\mu = \mu(T)$ is sufficient to cause the ratio $\mu_b|_r/\mu$ to decrease. It is interesting to note that the vibrational and rotational contributions are roughly equal at low temperatures whereas the rapid decrease in $Z_v$ causes the rotational contribution to dominate at higher temperatures.

## IV. FLUIDS HAVING LARGE BULK VISCOSITIES

We now consider fluids having bulk viscosities which are large compared to their shear viscosities. The first fluid considered is molecular hydrogen $H_2$ which has a characteristic vibrational temperature of approximately 6000 K. Thus, at the temperatures considered here, the primary contribution to the bulk viscosity will be due to the rotational mode. Rotational relaxation in hydrogen is particularly slow due to the low moment of inertia of the $H_2$ molecule. The resultant rotational energy levels are therefore widely spaced compared to heavier molecules such as $N_2$ and $O_2$. As a result, $H_2$ requires 200 or more collisions to establish equilibrium which is considerably more than the 5–10 collisions for $N_2$. Herzfeld and Litovitz[3] report values of $\alpha/\alpha_{cl}$ for $H_2$, where $\alpha$ is the measured acoustic absorption coefficient and $\alpha_{cl}$ is the $\mu_b = 0$ absorption coefficient, of 20–30 near room temperature which yields values of 36–55 for $\mu_b/\mu$. Here we have chosen the more recent data

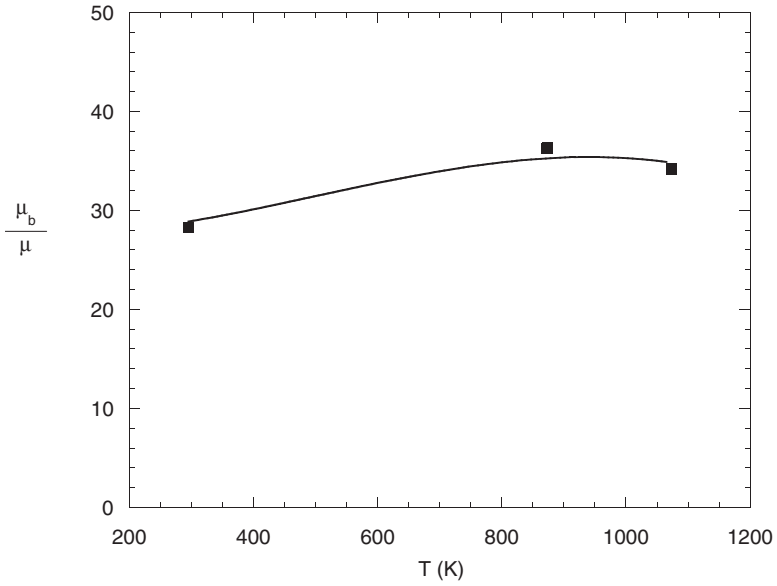


FIG. 5. Temperature variation of $\mu_b/\mu$ of $H_2$. The solid line denotes our curve-fit and the symbols denote values based on Winter and Hill's[40] data for $p\tau_r$.

of Winter and Hill[40] who report values of $p\tau_r$ for temperatures of 295 K, 873 K, and 1073 K. Their data were fit to a linear $p\tau_r$ vs $T$ relation

$$p\tau_r = a + bT,$$

where $a = 1.822 \times 10^{-4}$ kg/(m s) and $b = 4.641 \times 10^{-6}$ kg/(m s K). We also fit Winter and Hill's data to a power-law for $p\tau_r$, but the exponent of $T$ was very close to one and the simpler linear variation gives essentially the same results for $\mu_b/\mu$. We have plotted the resultant variation of $\mu_b/\mu$ vs $T$ for $H_2$ in Figure 5. We have also included the viscosity ratios computed based on Winter and Hill's discrete data. The values of $\mu_b/\mu$ are seen to be somewhat lower than those based on the older data reported by Herzfeld and Litovitz,[3] but nevertheless yield $\mu_b \approx 30\ \mu$ in the vicinity of room temperature. Our calculations show that $\mu_b$ increases monotonically from $\approx 25 \times 10^{-5}$ kg/(m s) at 295 K to $\approx 72 \times 10^{-5}$ kg/(m s) at 1073 K. However, the increase in $\mu_b$ is slower than the increase in $\mu$ with increasing $T$ resulting in a local maximum in $\mu_b/\mu$ at 941 K.

In the remainder of this section we consider fluids having a vibrational characteristic temperature which is low enough to result in the vibrational mode being active at room temperature. The first set of fluids to be considered is methane ($CH_4$), acetylene ($C_2H_2$), ethylene ($C_2H_4$), and cyclopropane (c-$C_3H_8$). Data for the vibrational relaxation times for each fluid were taken from Wang and Springer[49] who provided comparisons to previous studies and curve-fits for the values of $p\tau_v$. These fits were of the form of the Landau-Teller law and can be written as

$$p\tau_v = A \exp\left(\frac{B}{T^{\frac{1}{3}}}\right), \tag{30}$$

where

$$A = 429.3 \times 10^{-5}\,\text{kg/(m s)},\ B = 21.07(\text{K})^{\frac{1}{3}} \text{ for methane,}$$
$$A = 1086 \times 10^{-5}\,\text{kg/(m s)},\ B = 5.913(\text{K})^{\frac{1}{3}} \text{ for cyclopropane,}$$
$$A = 26.84 \times 10^{-5}\,\text{kg/(m s)},\ B = 22.29(\text{K})^{\frac{1}{3}} \text{ for acetylene,}$$
$$A = 39.42 \times 10^{-5}\,\text{kg/(m s)},\ B = 26.09(\text{K})^{\frac{1}{3}} \text{ for ethylene.}$$

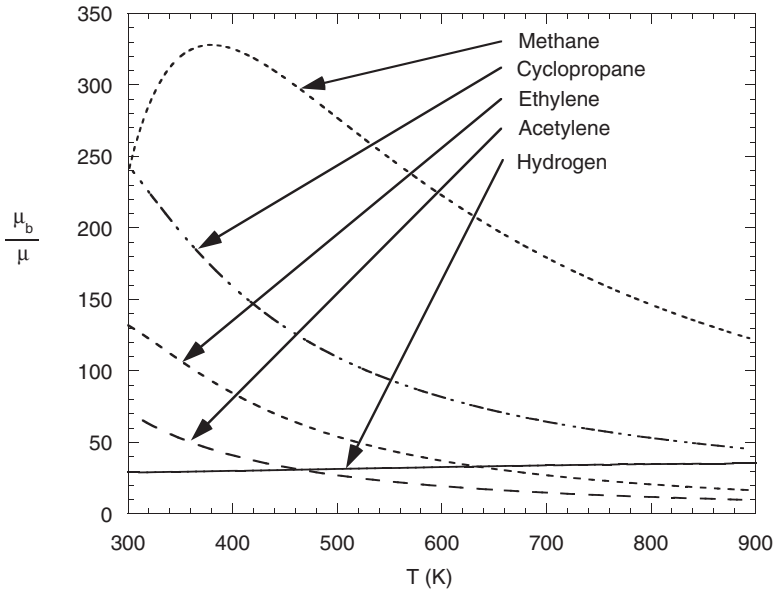


FIG. 6. Temperature variation of $\mu_b/\mu$ for selected fluids having bulk viscosities which are large compared to their shear viscosities.

When the values of $p\tau_v$ are substituted in (14) we obtain the temperature variations of $\mu_b/\mu$ plotted in Figure 6. For reference, we have also included the variation of $H_2$ in this figure.

Because of the strong decay of $p\tau_v$ with temperature inherent in the Landau-Teller variation (30), compounded with the increase in $\mu$ with increasing temperature, the values of $\mu_b$ and $\mu_b/\mu$ decrease monotonically with increasing temperature for ethylene, cyclopropane, and acetylene. However, methane shows a local maximum in both $\mu_b$ and $\mu_b/\mu$ at $\approx$450 K for $\mu_b$ and 378 K for $\mu_b/\mu$. The explanation for this non-monotone behavior can be seen by an inspection of the computed values of the coefficient (19). As pointed out in Sec. II, $\Delta \to 0$ near 257 K leading to the local maximum seen in Figure 6. We note that the magnitude of the slope of $\mu_b$ of ethylene also becomes relatively small at 300 K. If we employ (30) to compute $\mu_b$ for ethylene at temperatures slightly less than 300 K we find that ethylene also exhibits a non-monotone variation in $\mu_b$ with $T$. We note that use of the data of Holmes and Stott[50] for ethylene also gives rise to a local maximum in $\mu_b$ and $\mu_b/\mu$. In each case the reason for the local maximum is the decrease in $c_v\big|_v$ and $\Delta$ which overwhelms the increase in $p\tau_v$ as $T$ decreases.

Because $\mu_b\big|_v$ will always vanish as $c_v\big|_v \to 0$ and, at large temperatures, the variation of $\mu_b\big|_v$ is controlled by the strong decrease associated with the Landau-Teller law, we conclude that the vibrational contribution to $\mu_b$ will have a local maximum. Because the rotational component of the bulk viscosity is always present, the total bulk viscosity will be given by the gradually increasing rotational component at temperatures so low that $c_v\big|_v \approx 0$. We have sketched the expected qualitative behavior of $\mu_b$ in Figure 7.

In Figure 8 we have plotted the variation of $\mu_b/\mu$ of chlorine ($Cl_2$), fluorine ($F_2$), nitrous oxide ($N_2O$), sulfur hexafluoride ($SF_6$), and carbon tetrafluoride ($CF_4$). Each plot is based solely on the vibrational contribution to $\mu_b$. The bulk viscosity for $Cl_2$ was computed using the curve-fit provided by Hurly.[51] When cast in terms of $p\tau_v$ the fit for $Cl_2$ reads

$$p\tau_v = 0.7418 \times 10^{-5} T e^{\frac{1128.9}{T}}, \tag{31}$$

where $p\tau_v$ is in kg/(m s), $T$ is in degrees Kelvin and the formal range of validity is 260–440 K. Vibrational relaxation times for chlorine have been obtained by a number of other authors. We have compared the values of $\mu_b/\mu$ based on (31) to those based on the experimental data provided by Smiley and Winkler,[52] Eucken and Becker,[53] and Schultz[54] in Figure 9. In each case, the data were taken from Smiley and Winkler's Figure 6. Inspection of Figure 9 reveals that Hurly's more recent

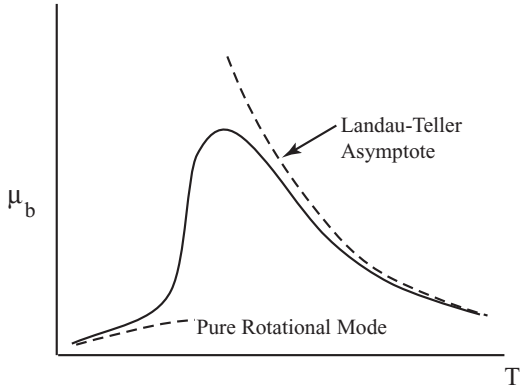


FIG. 7. Sketch of typical temperature variation of the bulk viscosity.

experiments yield $\mu_b \approx 440\ \mu$ at 300 K whereas the older data correspond to considerably larger values of $p\tau_v$ and therefore $\mu_b/\mu$. For example, Eucken and Becker's data are about 50% larger than that of Hurly over roughly the same temperature range.

For $F_2$ we used the curve-fit of Diebold, Santoro, and Goldsmith[55] which can be written in the form (30) with

$$A = 9.502 \times 10^{-5}\,\text{kg/(m s)},\quad B = 65.20(\text{K})^{\frac{1}{3}} \tag{32}$$

and should be formally valid in the range 500–1300 K. Here we refer the reader to Diebold, Santoro, and Goldsmith's Eq. (4) and their Figure 3 for an indication of the scatter of their results. Because the formal lower limit of the validity of (32) is 500 K, it is of interest to determine what can be said about the values of $\mu_b$ at room temperature. In Figure 3 of their report, Diebold, Santoro, and Goldsmith extend their Landau-Teller fit to lower temperatures yielding reasonable agreement with

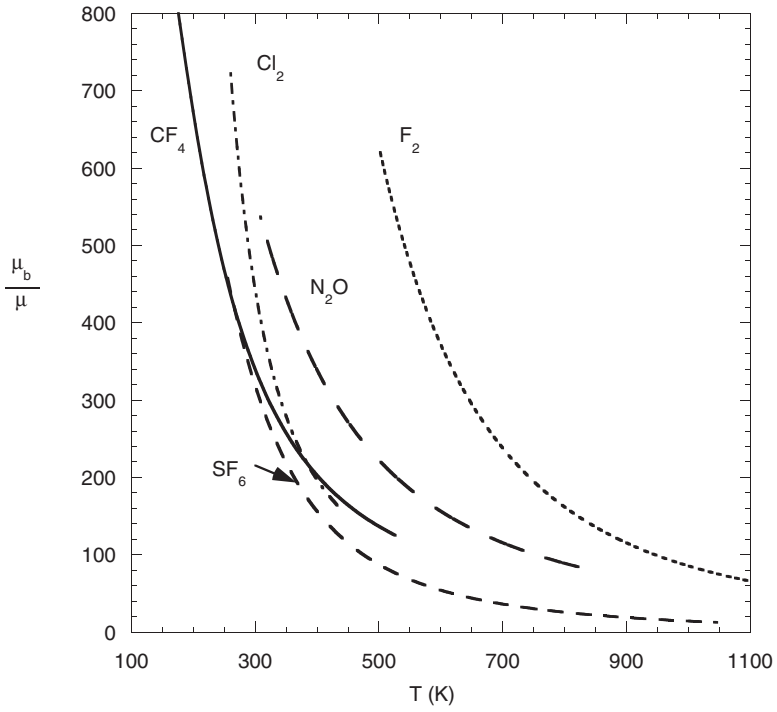


FIG. 8. Temperature variation of $\mu_b/\mu$ for selected fluids having large bulk viscosity.

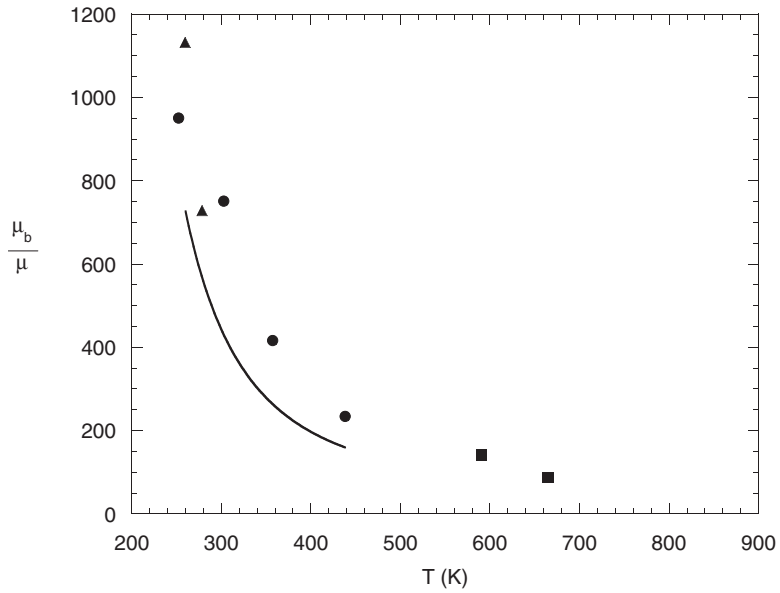


FIG. 9. Comparison of $\mu_b/\mu$ for $Cl_2$ to the results of earlier studies. The solid line denotes our fit based on the formula by Hurly,[51] ■ denotes values based on the experiments of Smiley and Winkler,[52] • denotes values based on the experiments of Eucken and Becker,[53] and ▲ denotes values based on the work of Schultz.[54]

the data of Shields.[56] In particular, the difference in $p\tau_v$ is well within the suggested scatter of Diebold, Santoro, and Goldsmith's experiment. We assume that Shields' data for $F_2$ correspond to a pressure of 1 atm and obtain a result for $p\tau_v$ which is approximately that plotted by Diebold, Santoro, and Goldsmith[55] in their Figure 3. In Figure 10 we have plotted the values of $\mu_b/\mu$ based on (32) and (30), but extended to 300 K along with values of $\mu_b/\mu$ based on Shields' data. Again, the newer data yield a lower value of $\mu_b$. Nevertheless, this extrapolated, but conservative, estimate suggests that $\mu_b > 2200\ \mu$ at 300 K.

The bulk viscosities for sulfur hexafluoride were computed using the data of Holmes and Stott[50] and the curve-fit provided by Breshears and Blair.[57] The latter authors concluded that their experimental data conformed to the Landau-Teller law and could be represented by (30) with

$$A = 0.2959\,\text{kg/(m s)}\,,\ \ B = 38(\text{K})^{\frac{1}{3}},$$

which was expected to be valid for $450\,\text{K} \le T \le 1050\,\text{K}$. In the fit used here, only the data from 251.15 K to 418.15 K of Holmes and Stott's report were included. To generate a single fit to both data sets we used Breshears and Blair's curve-fit to generate discrete "data" points and then fit the combined set to an equation of the form

$$p\tau_v = A\,\exp\left[\frac{B}{T^{\frac{1}{3}}} + \frac{C}{T^{\frac{2}{3}}}\right]. \tag{33}$$

The number of discrete points corresponding to Breshears and Blair's data was taken to be equal to the number of points used from Holmes and Stott. The resultant values of the constants in (33) were

$$A = 0.2064\,\text{kg/(m s)},\ \ B = 121(\text{K})^{\frac{1}{3}},\ \ C = -339(\text{K})^{\frac{2}{3}}.$$

A comparison of the bulk viscosities based on our fit, Breshears and Blair's fit, and the discrete data of Holmes and Stott is plotted in Figure 11. As can be seen, our fit agrees very well with the experimental data at 300 K. The maximum difference between our fit and the experimental data is about 13% at 418 K.

The plot for $CF_4$ is based on a curve-fit to the data of Corran *et al.*[58] and Ewing and Trusler.[59] All the data of Ewing and Trusler[59] were used. We assumed that the data of Corran *et al.* correspond to 1 atm and we also omitted the point at 588 K in our fit. This last point appeared to be an anomaly

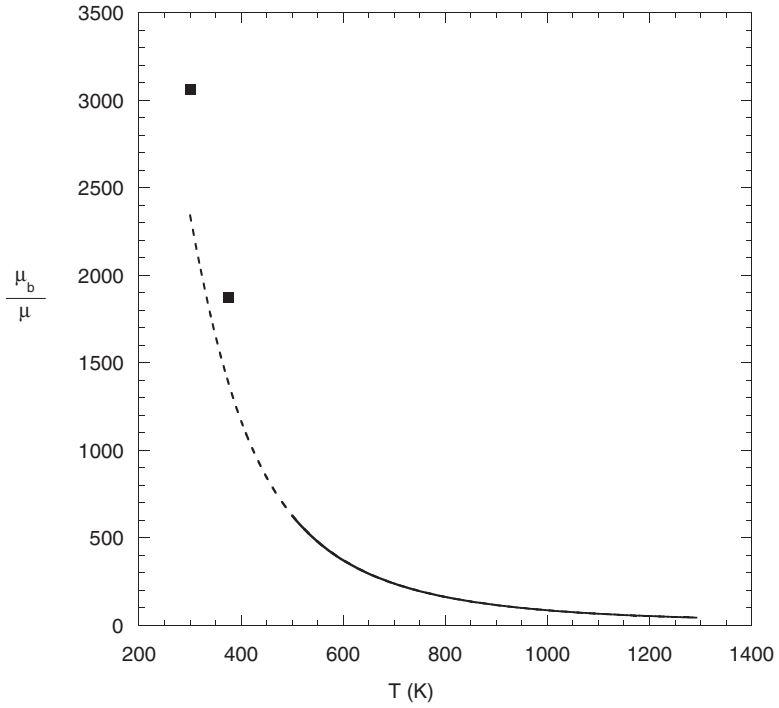


FIG. 10. Comparison of $\mu_b/\mu$ for $F_2$ to the data of Shields.[56] The solid line represents our curve-fit, the dashed line represents the extension of our fit to 300 K, and the symbols denote values based on the experiments of Shields.[56]

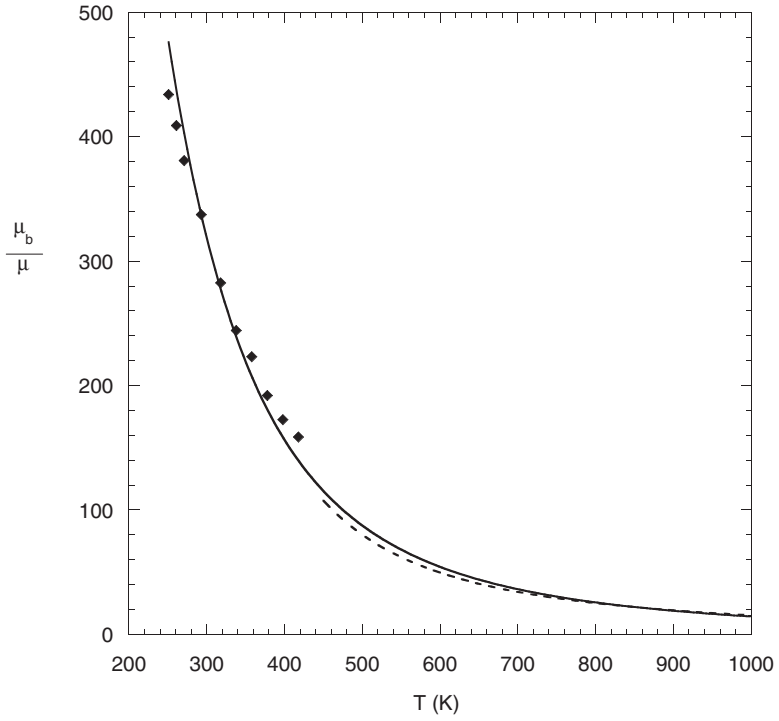


FIG. 11. Composite curve-fit of temperature variation for $SF_6$. Solid line represents our curve-fit, symbols are based on the discrete data of Holmes and Stott,[50] and the dashed line represents the curve-fit provided by Breshears and Blair.[57]

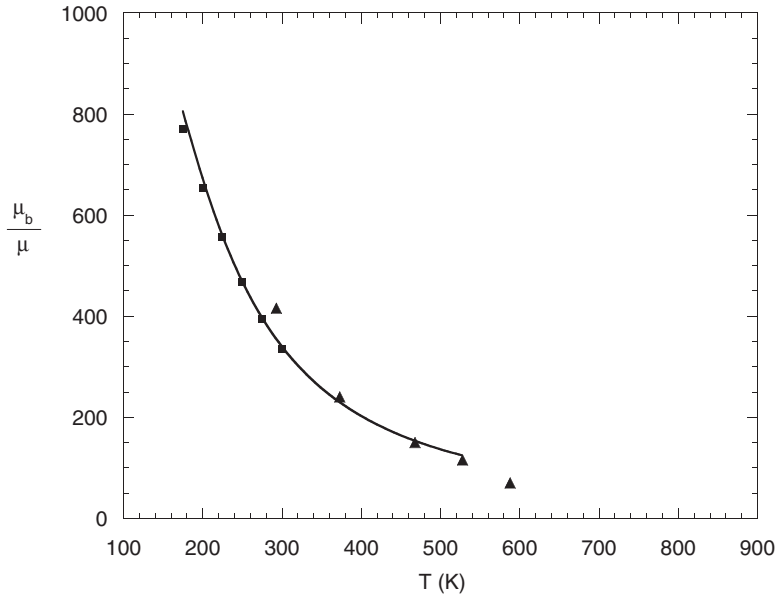


FIG. 12. Composite curve-fit of temperature variation of $\mu_b/\mu$ for $CF_4$. The solid line represents our curve-fit, ■ denotes the values based on the data of Ewing and Trusler,[59] and ▲ denotes values based on the data of Corran *et al.*[58]

compared to the rest of Corran *et al.*'s data. Our fit was of the Landau-Teller type, i.e., (30), with

$$A = 497.8\,\text{kg/(m s)} \text{ and } B = 17.9(\text{K})^{\frac{1}{3}},$$

which is expected to be valid from 175 K to 518 K. A comparison of our fit to the discrete data is provided in Figure 12. This plot also includes the anomalous point at 588 K. Our fit agrees quite well with the data of Ewing and Trusler[59] near 300 K, whereas there is about a 14% discrepancy between our fit and Corran *et al.*'s[58] data point at 293 K.

The variation of $\mu_b/\mu$ for nitrous oxide ($N_2O$) plotted in Figure 8 was computed using the shock tube data of Simpson, Bridgman, and Chandler[60] who carefully accounted for a dependence of the results on departures from equilibrium. The authors compared their results to previous investigations including the well known study of Griffith, Brickl, and Blackman.[61] Simpson, Bridgman, and Chandler[60] reported their data as a single curve which presumably was a fit to discrete data. Using graph-digitizer software, we extracted $(p\tau_v,\ T^{\frac{1}{3}})$ points from their Figure 3 and, because their curve did not conform well to the Landau-Teller law, we then fit their points to a power-law of the form

$$p\tau_v = (p\tau_v)_{\text{ref}} \left(\frac{T}{T_{\text{ref}}}\right)^n, \tag{34}$$

where $(p\tau_v)_{\text{ref}} = 0.05305$ kg/(m s), $T_{\text{ref}} = 500$ K, and $n = -1.178$. Our fit is expected to be valid over the same range covered by Simpson, Bridgman, and Chandler,[60] i.e., 320–850 K.

The final fluid to be considered is carbon dioxide ($CO_2$) which has historically been regarded as having $\mu_b/\mu = \text{O}(10^3)$. The data used for our estimates are the relaxation time data of Simpson, Bridgman, and Chandler[62] who accounted for departures from equilibrium on the reported value of the relaxation time, the sensitivity of the test gas to trace amounts of water vapor, and made comparisons to previous investigations. As in the case of $N_2O$, the authors report their results only as a single curve. We followed the same procedure as for $N_2O$ and found that their curve could be represented by a power-law of the form (34) with

$$(p\tau_v)_{\text{ref}} = 0.19152\ \text{kg/(m s)},\ T_{\text{ref}} = 800\,\text{K},\ n = -1.353$$

which should be valid for $296\,\text{K} \le T \le 1711\,\text{K}$. We have plotted the values of $\mu_b/\mu$ based on our curve-fit along with the values based on the points taken from Simpson, Bridgman, and Chandler's Figure 5 in Figure 13. We note that value of the bulk viscosity based on our power-law at 296.3 K

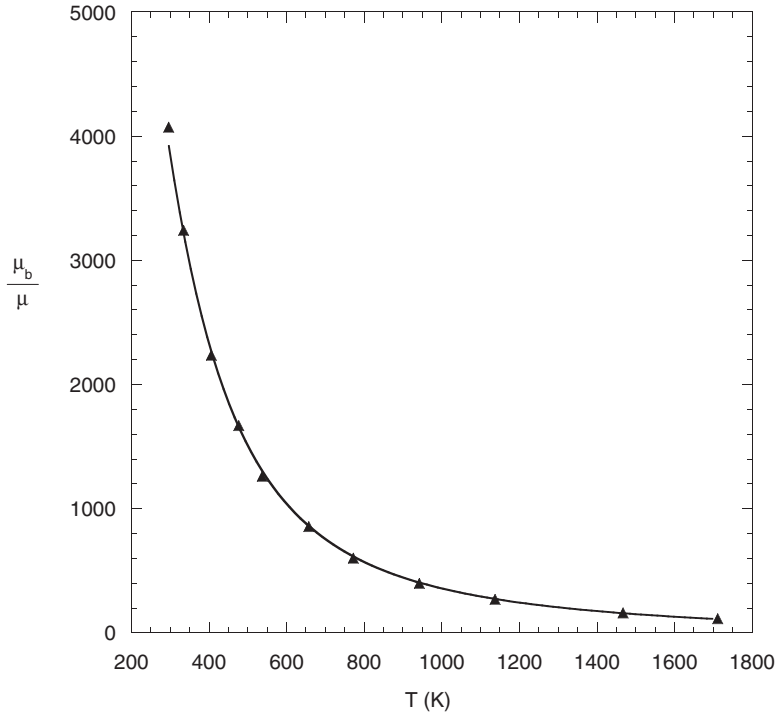


FIG. 13. Temperature variation of $\mu_b/\mu$ for $CO_2$. The solid line represents our curve-fit and the symbols are values based on data taken from Simpson, Bridgman, and Chandler.[62]

was 3922 $\mu$ whereas the value based on the data taken from Simpson, Bridgman, and Chandler's Figure 5 was 4073 $\mu$ for a difference of ≈3.7%; this is the largest discrepancy in Figure 13.

At 300 K, we find that our fit yields $p\tau_v \approx 0.72$ kg/(m s) which is only about 5% higher than the value of $p\tau_v$ used by Emanuel.[30] At 300 K, our estimates yield

$$c_v \approx 3.48R,\ \mu \approx 1.52 \times 10^{-5}\,\text{kg/(m s)},\ \mu_b \approx 5845 \times 10^{-5}\,\text{kg/(m s)}$$

yielding a ratio $\mu_b/\mu = 3849$ which is about 8% larger than an estimate for $\mu_b/\mu$ obtained by using Emanuel's data and the Planck-Einstein formula for the vibrational specific heat.

## V. PREDICTIONS OF THE GENERAL SIZE OF THE BULK VISCOSITY

The estimates for $\mu_b$ found in Secs. III and IV have ranged from $\mu_b = O(\mu)$ to $\mu_b = O(10^3\mu)$. In the design of experiments, power systems, and other technologies, it is useful to have a simple method for the estimation of the general size of $\mu_b/\mu$. Because the variability of $\mu_b$ from fluid to fluid is primarily due to the variability of the relaxation time, we believe that the Lambert-Salter[63] empirical correlation can provide a reasonable guide to the size of the ratio $\mu_b/\mu$.

The Lambert-Salter correlation relates the collision number $Z_{10}$ to the characteristic temperature corresponding to the lowest vibrational mode as follows:

$$\log_{10} Z_{10} = K\theta_v, \tag{35}$$

where $K$ is a constant taken to depend on the number of hydrogen atoms comprising the molecule and the temperature at which $Z_{10}$ is evaluated, typically taken to be 300 K. The value of $K$ for molecules having no hydrogen atoms is observed to be larger than that corresponding to molecules having two or more hydrogen atoms. An illustration of the Lambert-Salter correlation is provided in Figure 14. The values of $Z_{10}$ were computed from our estimates of $\mu_b/\mu$ at 300 K and (10) for *n*-butane, *n*-pentane, dimethylpropane, acetylene, ethylene, cyclopropane, and methane. The straight line fits seen in Figure 14 are based on a least-squares fit to the slope; because $Z_{10} \geq 1$, we

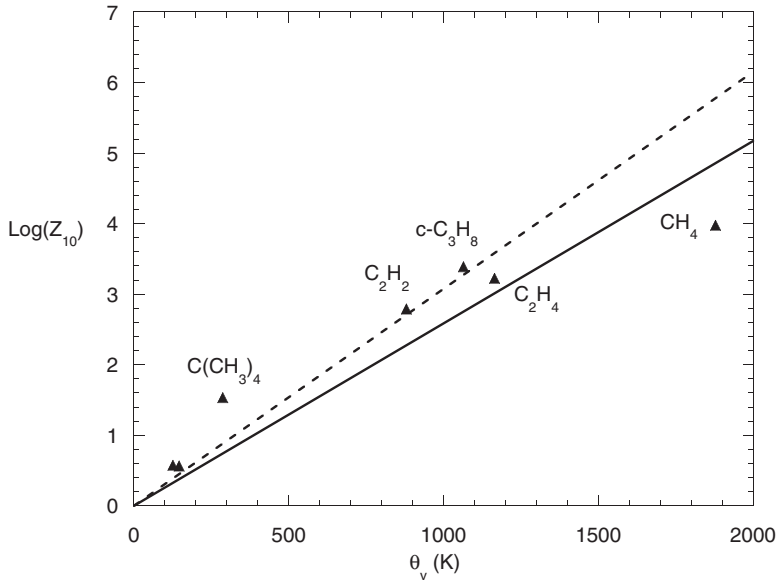


FIG. 14. Lambert-Salter plot for molecules containing two or more hydrogen molecules. The two substances having $\log(Z_{10}) < 1$ are n-butane (n-$C_4H_{10}$) and n-pentane (n-$C_5H_{12}$). The dashed line is a straight line fit to the data excluding $CH_4$ and the solid line is a straight line fit including $CH_4$.

follow Lambert and Salter[63] and Lambert[35] in fixing $\log_{10}Z_{10} = 0$ at $\theta_v = 0$. As seen in the studies of Lambert,[35] methane falls below the line determined by the general grouping. Thus, we have provided straight line fits to our own more limited data set both including and excluding methane. The corresponding values of $K$ were found to be $2.6 \times 10^{-3}(\mathrm{K})^{-1}$ and $3.1 \times 10^{-3}(\mathrm{K})^{-1}$, respectively.

The variation of $\mu_b/\mu$ with $\theta_v$ at fixed temperature can be anticipated by considering the ratio

$$\frac{\mu_b|_v}{\mu_{HS}} = \frac{4}{5}\Delta Z_v, \tag{36}$$

where $\mu_{HS}$ is the hard sphere approximation (6) for the shear viscosity. If we combine (35) with (10), we have

$$Z_v = \frac{10^{K\theta_v}}{1 - e^{-\frac{\theta_v}{T}}},$$

which is seen to have a local minimum at $\theta_v \approx 115\mathrm{K}$ if we use $T = 300\mathrm{K}$ and $K \approx 3.1 \times 10^{-3}(\mathrm{K})^{-1}$. If we assume that $\Delta = \Delta(\theta_v)$ at fixed temperature, it is reasonable to conclude that

$$\frac{\mu_b|_v}{\mu_{HS}} = f(\theta_v).$$

If we use the more accurate estimate (16) for the viscosity, we must include the collision integral (18) in the numerator of (36). Because $\Omega = \Omega(T_\epsilon)$ at fixed temperature and $T_\epsilon$ is independent of $\theta_v$, a pure correlation of $\mu_b/\mu$ with $\theta_v$ is not strictly possible. However, the numerical value of $\Omega$ does not vary strongly from fluid to fluid and we would expect that some simple trend could nevertheless be observed. As partial support for this conjecture, we have plotted our computed values of $\log_{10}(\mu_b/\mu)$ against $\theta_v$ for the same fluids as were used in Figure 14 in Figure 15. Except for methane we see a clear increase in $\mu_b/\mu$ with $\theta_v$. The relatively low value of $\log_{10}(\mu_b/\mu)$ of methane is primarily due to the anomalous behavior of $CH_4$ with respect to the Lambert-Salter plot of Figure 14. A second contributing factor is the fact that the vibrational mode is becoming deactivated in the vicinity of 300 K. This decrease in $c_v|_v$ and $\Delta$ can be seen in Figure 1 and gave rise to the non-monotone variation of $\mu_b/\mu$ with $T$ in Figure 6.

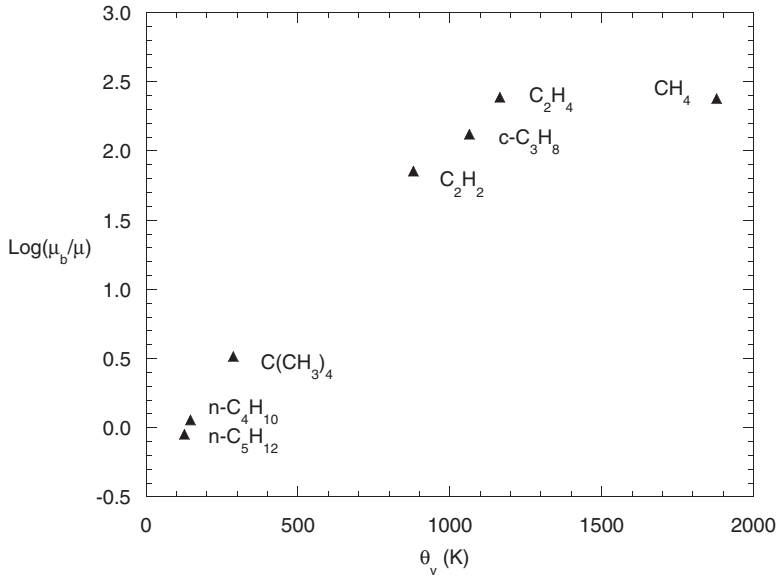


FIG. 15. Variation of $\mu_b/\mu$ with characteristic temperature of vibration at 300 K.

We have also verified that our calculations are consistent with Lambert and Salter's observation that fluids having no hydrogen atoms have a larger $K$-value and therefore have larger values of $Z_{10}$ at the same value of $\theta_v$. The estimates of $\mu_b/\mu$ for fluids having no hydrogen atoms were also seen to be larger than those having hydrogen molecules at the same $\theta_v$.

In conclusion, we believe that, at a given temperature, $\mu_b/\mu$ can generally be regarded as an increasing function of $\theta_v$. Fluids having no hydrogen atoms, e.g., $CO_2$, $CF_4$, $SF_6$, etc., are expected to have higher values of $\mu_b/\mu$ for the same value of $\theta_v$ than fluids containing hydrogen atoms. However, this trend will become invalid at sufficiently large values of $\theta_v$, i.e., when $T/\theta_v \to 0$. As $\theta_v \to \infty$, $\Delta \to 0$ and the vibrational modes become inactive, i.e., $\mu_b\big|_v \to 0$. Thus, there will be a local maximum in the $\mu_b\big|_v/\mu$ (or $\log_{10} \mu_b\big|_v/\mu$) vs $\theta_v$ curve.

In cases where $\mu_b\big|_v \ll \mu_b\big|_r$, i.e., $T \ll \theta_v$, the rotational contribution to $\mu_b$ is dominant and the general size of $\mu_b$ is $O(\mu)$; an important exception is $H_2$ for which $\mu_b$ is roughly 30 times $\mu$ at room temperature.

As discussed by Lambert and Salter[63] and Lambert,[35] polar fluids are expected to possess a more complicated behavior. However, if the strong dipole forces are large enough, the energy transfer will be highly efficient so that we would expect $\mu_b$ to be $O(\mu)$ for polar fluids. We expect that exceptions will occur if the energy associated with the dipole is weak compared to the kinetic energy at the temperature in question; examples are expected to include methyl chloride ($CH_3Cl$) and methyl fluoride ($CH_3F$) which, according to Table 3.5 of Lambert,[35] can have values of $Z_{10}$ on the order of acetylene or higher at 300 K.

## VI. SUMMARY

The primary objective of the present study is to provide estimates of the bulk viscosity (1) of dilute polyatomic gases using Tisza's formula (3) or (12)–(14) combined with published measurements of the vibrational and rotational relaxation times. Unlike the shear viscosities, the bulk viscosities can have a wide range of numerical values and temperature variations, even in the ideal gas limit. The discussion and analysis presented here suggests that the temperature variation of the bulk viscosity will always have a local maximum. At sufficiently low temperatures, the vibrational mode is deactivated and the bulk viscosity is due to the relaxation of the rotational mode typically yielding a bulk viscosity which is $O(\mu)$ and is gradually increasing with temperature. At sufficiently high temperatures, the vibrational mode is activated and the bulk viscosity is characterized by the

strong decay with temperature associated with the Landau-Teller theory. Hence, at least one local maximum must occur.

The largest values of the maximum value of $\mu_b/\mu$ are likely to occur when the characteristic temperature of vibration is considerably larger than that where dipole moments or attractive forces are non-negligible. In this case, the local maximum will occur as the vibrational mode is activated and marks the transition between the Landau-Teller region and the region where the bulk viscosity is primarily due to its rotational contribution. If, on the other hand, $\theta_v$ is so low that attractive and dipole forces play a role after the vibrational modes are activated, the equilibration of the vibrational energy will be efficient and the resultant local maximum in $\mu_b$ will typically be $O(\mu)$.

In Sec. V we have employed the Lambert-Salter correlation to suggest that the numerical value of $\mu_b/\mu$ at a given temperature can be inferred by a knowledge of $\theta_v$. For example, it appears that fluids having similar numbers of hydrogen atoms and which have larger values of $\theta_v$ will also have larger values of $\mu_b/\mu$ at the same temperature. The limitation of this tendency occurs when the chosen temperature is small compared to $\theta_v$ resulting in a deactivation of the vibrational mode. Although we provide no detailed supporting data, we believe that it is reasonable to conjecture that the variation of $\mu_b/\mu$ with $\theta_v$ at constant temperature will always have a local maximum.

The general order of magnitude of $\mu_b/\mu$ for substances such as $N_2$, $CO_2$, $N_2O$, and $H_2$ at room temperature is in reasonable agreement with the estimates provided in previous investigations. A contribution of the present study is to establish explicit estimates of $\mu_b$ for a wider range of fluids than considered previously. In doing so, it is seen that many common fluids, including diatomic gases, can have bulk viscosities which are hundreds to thousands of times larger than their shear viscosities.

The primary factor determining the accuracy of our estimates is the accuracy of the published relaxation times. Due to the difficulty of the measurements, scatter in excess of 10% is commonly observed. An important contribution to the determination of $\mu_b$ is the refinement of estimates for the relaxation times, particularly $H_2O$ and other fluids of technological interest.

## ACKNOWLEDGMENTS

The author would like to thank Ms. E. Via for assistance in data collection and curve-fitting. This work was supported by National Science Foundation (NSF) grant CBET-0625015.

[1] L. Tisza, "Supersonic absorption and Stokes' viscosity relation," Phys. Rev. **61**, 531 (1942).
[2] R. E. Graves and B. M. Argrow, "Bulk viscosity: past to present," Int. J. Thermophys. **13**, 337 (1999).
[3] K. F. Herzfeld and T. A. Litovitz, *Absorption and Dispersion of Ultrasonic Waves* (Academic, New York, 1959).
[4] S. M. Karim and L. Rosenhead, "The second coefficient of viscosity of liquids and gases," Revs. Modern Phys. **24**, 108 (1952).
[5] P. A. Thompson, *Compressible-Fluid Dynamics* (McGraw-Hill, New York, 1972).
[6] H. M. Curran, "Use of organic working fluids in Rankine engines," J. Energy **5**, 218 (1981).
[7] S. Devotta and F. A. Holland, "Comparison of theoretical Rankine power cycle performance for 24 working fluids," Heat Recovery Syst. **5**, 503 (1985).
[8] J. Yan, "On thermodynamic cycles with non-azeotropic mixtures as working fluids," Ph.D. dissertation, (Royal Institute of Technology, Stockholm, Sweden, 1991).
[9] T. C. Hung, T. Y. Shai, and S. K. Wang, "A review of organic Rankine cycles (ORCs) for the recovery of low-grade waste heat," Energy **22**, 661 (1997).
[10] B.-T. Liu, K.-H. Chien, and C.-C. Wang, "Effect of working fluids on organic Rankine cycle for waste heat recovery," Energy **29**, 1207 (2004).
[11] D. Wei, X. Lu, Z. Lu, and J. Gu, "Performance analysis and optimization of organic Rankine cycle (ORC) for waste heat recovery," Energy Convers. Manage. **48**, 1113 (2007).
[12] B. Saleh, G. Koglbauer, M. Wendland, and J. Fischer, "Working fluids for low-temperature organic Rankine cycles," Energy **32**, 1210 (2007).
[13] A. Shuster, S. Karellas, and R. Aumann, "Efficiency optimization potential in supercritical organic Rankine cycles," Energy **35**, 1033 (2010).
[14] V. Dostal, M. J. Driscoll, P. Hejzlar, and N. E. Todreas, "A supercritical $CO_2$ Brayton cycle for advanced reactor applications," Trans. Am. Nucl. Soc. **85**, 110 (2001).
[15] V. Dostal, M. J. Driscoll, P. Hejzlar, and N. E. Todreas, "Component design for a supercritical $CO_2$ Brayton cycle," Trans. Am. Nucl. Soc. **87**, 536 (2002).
[16] V. Dostal, "A supercritical carbon dioxide cycle for next generation nuclear reactors," Ph.D. dissertation (Massachusetts Institute of Technology, Cambridge, MA, 2004).

[17] A. Moisseytsev, "Passive load follow analysis of the STAR-LM and STAR-H2 systems," Ph.D. dissertation (Texas A&M University, College Station, TX, 2003).
[18] A. Moisseytsev and J. J. Sienicki, "Investigation of alternative layouts for the supercritical carbon dioxide Brayton cycle for a sodium-cooled fast reactor," Nucl. Eng. Des. **239**, 1362 (2009).
[19] J. Sarkar, "Second law analysis of supercritical $CO_2$ recompression Brayton cycle," Energy **34**, 1172 (2009).
[20] J. Sarkar, "Thermodynamic analyses and optimization of a recompression $N_2O$ Brayton power cycle," Energy **35**, 3422 (2010).
[21] W. K. Anderson, "Numerical study of the aerodynamic effects of using sulfur hexafluoride as a test gas in wind tunnels," NASA Technical Paper 3086, 1991.
[22] W. K. Anderson, "Numerical study on using sulfur hexafluoride as a wind tunnel test gas," AIAA J. **29**, 2179 (1991).
[23] J. B. Anders, "Heavy gas wind tunnel research at Langley Research Center," ASME Paper 93-FE-5, 1993.
[24] J. W. Tom and P. G. Debenedetti, "Particle formation with supercritical fluids—a review," J. Aerosol Sci. **22**, 555 (1991).
[25] C. A. Eckert, B. L. Knutson, and P. G. Debenedetti, "Supercritical fluids as solvents for chemical and materials processing," Nature (London) **383**, 313 (1996).
[26] M. Turk, B. Helfgen, P. Hils, R. Lietzow, and K. Schaber, "Micronization of pharmaceutical substances by rapid expansion of supercritical solutions (RESS): experiments and modeling," Part. Part. Syst. Charact. **19**, 327 (2002).
[27] S. Chapman and T. G. Cowling, *Mathematical Theory of Non-Uniform Gases* (Cambridge University Press, London, 1970).
[28] G. J. Prangsma, A. H. Alberga, and J. J. M. Beenakker, "Ultrasonic determination of the volume viscosity of $N_2$, CO, $CH_4$ and $CD_4$ between 77 and 300 K," Physica **64**, 278 (1973).
[29] F. S. Sherman, "A low-density wind-tunnel study of shock-wave structure and relaxation phenomena in gases,", NACA TN-3298, 1955.
[30] G. Emanuel, "Effect of bulk viscosity on a hypersonic boundary layer," Phys. Fluids A **4**, 491 (1992).
[31] J. G. Parker, "Rotational and vibrational relaxation in diatomic gases," Phys. Fluids **2**, 449 (1959).
[32] R. N. Schwartz, Z. I. Slawsky, and K. F. Herzfeld, "Calculation of vibrational relaxation times in gases," J. Chem. Phys. **10**, 1591 (1952).
[33] R. N. Schwartz and K. F. Herzfeld, "Vibrational relaxation in gases (three-dimensional treatment)," J. Chem. Phys. **22**, 767 (1954).
[34] F. I. Tanczos, "Calculation of vibrational relaxation times of the chloromethanes," J. Chem. Phys. **25**, 439 (1956).
[35] J. D. Lambert, *Vibrational and Rotational Relaxation in Gases* (Clarendon, Oxford, 1977).
[36] R. C. Reid, J. M. Prausnitz, and B. E. Poling, *The Properties of Gases and Liquids*, 4th ed. (McGraw-Hill, New York, 1987).
[37] R. C. Reid, J. M. Prausnitz, and T. K. Sherwood, *The Properties of Gases and Liquids*, 3rd ed. (McGraw-Hill, New York, 1977).
[38] R. A. Svehla, "Estimated viscosities and thermal conductivities of gases at high temperatures," NASA TR R-132, 1962.
[39] G. Emanuel, "Bulk viscosity of a dilute polyatomic gas," Phys. Fluids **2**, 2252 (1990).
[40] T. G. Winter and G. L. Hill, "High-temperature ultrasonic measurements of rotational relaxation in hydrogen, deuterium, nitrogen, and oxygen," J. Acoust. Soc. Am. **42**, 848 (1967).
[41] M. B. Ewing, A. R. H. Goodwin, M. L. McGlashan, and J. P. M. Trusler, "Thermophysical properties of alkanes from speeds of sound determined using a spherical resonator: 1. Apparatus, acoustic model, and results for dimethylpropane," J. Chem. Thermodyn. **19**, 721 (1987).
[42] M. B. Ewing, A. R. H. Goodwin, and J. P. M. Trusler, "Thermophysical properties of alkanes from speeds of sound determined using a spherical resonator. 3. N-pentane," J. Chem. Thermodyn. **21**, 867 (1989).
[43] M. B. Ewing and A. R. H. Goodwin, "Thermophysical properties of alkanes from speeds of sound determined using a spherical resonator: 5. 2-methylbutane at temperatures in the range 260 K to 320 K and pressures in the range 2.8 kPa to 80.9 kPa," J. Chem. Thermodyn. **24**, 301 (1992).
[44] M. B. Ewing, A. R. H. Goodwin, M. L. McGlashan, and J. P. M. Trusler, "Thermophysical properties of alkanes from speeds of sound determined using a spherical resonator: 2. N-butane," J. Chem. Thermodyn. **20**, 243 (1988).
[45] M. B. Ewing and A. R. H. Goodwin, "Thermophysical properties of alkanes from speeds of sound determined using a spherical resonator: 4. 2-methylpropane at temperatures in the range 251 K to 320 K and pressures in the range 5 kPa to 114 kPa," J. Chem. Thermodyn. **23**, 1107 (1991).
[46] R. Holmes, G. R. Jones, and R. Lawrence, "Vibrational-rotation-translational energy exchange in some polyatomic molecules," Trans. Faraday Soc. **62**, 46 (1966).
[47] H. E. Bass, J. R. Olson, and R. C. Amme, "Vibrational relaxation in $H_2O$ vapor in the temperature range of 373-946 K," J. Acoust. Soc. Am. **56**, 1455 (1974).
[48] R. G. Keeton and H. E. Bass, "Vibrational and rotational relaxation of water vapor by water vapor, nitrogen, and argon at 500 K," J. Acoust. Soc. Am. **60**, 78 (1976).
[49] J. C. F. Wang and G. S. Springer, "Vibrational relaxation times in some hydrocarbons in the range 300–900 °K," J. Chem. Phys. **59**, 6556 (1973).
[50] R. Holmes and M. A. Stott, "Temperature dependence of vibrational relaxation times in cyclopropane, ethylene and sulfur hexafluoride," Br. J. Appl. Phys. **1**, 1331 (1968).
[51] J. J. Hurly, "Thermophysical properties of chlorine from speed-of-sound measurements," Int. J. Thermophys. **23**, 455 (2002).
[52] E. F. Smiley and E. H. Winkler, "Shock-tube measurements of vibrational relaxation," J. Chem. Phys. **22**, 2018 (1954).
[53] A. Eucken and R. Becker, "Excitation of intramolecular vibrations in gases and gas mixtures by collisions, based on measurements of sound dispersion," Z. Phys. Chem. **27**, 219 (1934).
[54] R. Schultz, "Über Hörschall geschwindigkeit und -dispersion in Chlor," Ann. Phys. **426**, 41 (1939).
[55] G. J. Diebold, R. J. Santoro, and G. J. Goldsmith, "Vibrational relaxation of fluorine by a shock tube schlieren method," J. Chem. Phys. **60**, 4170 (1974).

[56] F. D. Shields, "Thermal relaxation in fluorine," J. Acoust. Soc. Am. **34**, 271 (1962).
[57] W. D. Breshears and L. S. Blair, "Vibrational relaxation in polyatomic molecules: $SF_6$," J. Chem. Phys. **59**, 5824 (1973).
[58] P. G. Corran, J. D. Lambert, R. Salter, and B. Warburton, "Temperature dependence of vibrational relaxation times in gases," Proc. R. Soc., London **A244**, 212 (1958).
[59] M. B. Ewing and J. P. M. Trusler, "Speeds of sound in $CF_4$ between 175 and 300 K measured with a spherical resonator," J. Chem. Phys. **90**, 1106 (1989).
[60] C. J. S. M. Simpson, K. B. Bridgman, and T. R. D. Chandler, "Shock-tube study of vibrational relaxation in nitrous oxide," J. Chem. Phys. **49**, 509 (1968).
[61] W. Griffith, D. Brickl, and V. Blackman, "Structure of shock waves in polyatomic gases," Phys. Rev. **102**, 1209 (1956).
[62] C. J. S. M. Simpson, K. B. Bridgman, and T. R. D. Chandler, "Shock-tube study of vibrational relaxation in carbon dioxide," J. Chem. Phys. **49**, 513 (1968).
[63] J. D. Lambert and R. Salter, "Vibrational relaxation in gases," Proc. R. Soc., London **A253**, 277 (1959).